CHEMISTRY
A EUROPEAN JOURNAL

ChemPubSoc
Europe

DOI: 10.1002/chem.201204315

pH-Controlled Reversible Formation of a Supramolecular Hyperbranched Polymer Showing Fluorescence Switching

Bingran Yu,[a] Baoyan Wang,[a] Shuwen Guo,[a] Qian Zhang,[a] Xiaorui Zheng,[a] Haitao Lei,[a] Weisheng Liu,[a] Weifeng Bu,*[a] Yun Zhang,[b] and Xin Chen[b]

Abstract: A π-conjugated AB_2 monomer **1** with a dibenzo[24]crown-8 (DB24C8) ring and two secondary amine centres has been synthesised. Treatment of a solution of **1** in dichloromethane with trifluoroacetic acid (TFA) leads to protonation of the amine groups, and then the DB24C8 rings are threaded by the dialkylammonium ion centres of other monomer molecules, leading to the formation of a supramolecular hyperbranched polymer, TFA-**1**. Rather strong π–π stacking interactions between the conjugated cores are evident in this polymer. The supramolecular hyperbranched polymer (SHP) can be completely depolymerised by adding a slight excess of *N-tert*-butyl-*N*′,*N*′,*N*″,*N*″,*N*‴,*N*‴-hexamethylphosphorimidic triamide, tetrabutylammonium fluoride, or tetrabutylammonium acetate. The acid–base-controlled process induces a reversible change in the fluorescence intensities of the solutions due to the controllable presence of the π–π stacking interactions between the conjugated cores. This dynamic behaviour is significant with respect to "smart" supramolecular polymer materials.

Keywords: acid–base reaction · fluorescence switch · molecular recognition · supramolecular chemistry · π–π stacking

Introduction

Hyperbranched polymers adopt highly branched and globular architectures, are highly soluble in appropriate solvents, and have low melt and solution viscosities in comparison with their linear analogues.[1] They are usually synthesised in high yields by one-pot covalent polymerisation of AB_m monomers ($m \geq 2$). Alternatively, noncovalent connections of AB_m or other monomers can result in the formation of supramolecular hyperbranched polymers (SHPs).[2] The driving force behind such assembly processes is commonly based on host–guest recognition, and examples of this have involved crown ethers with viologen moieties,[2a] [60]fullerene with concave aromatic electron donors,[2b] and β-cyclodextrin with azophenyl[2c] and adamantyl[2d,e] groups. Such assemblies are usually considered to have a dynamic nature. However, rare examples show reversible polymerisation and depolymerisation in response to external stimuli.[2c] Despite progress in this area, SHPs built up of star-shaped π-conjugated monomers, which might hold great promise for applications in optoelectronic devices, have not hitherto been demonstrated.

The crown ether moiety of dibenzo[24]crown-8 (DB24C8) can host a dialkylammonium ion centre ($-CH_2NH_2^+CH_2-$) with a molar ratio of 1:1 driven by a cooperative combination of [N^+–H···O] and [C–H···O] hydrogen bonds and π–π stacking interactions.[3,4] This recognition motif has a high binding constant in CH_2Cl_2.[3c] Upon the addition of excess base to the solution, deprotonation of the ammonium recognition site occurs, and thus the pseudorotaxane complex dissociates. Subsequent addition of acid can completely restore the inclusion complex.[3d–g] Such acid–base-controllable switching occurs very rapidly. Alternatively, such a pseudorotaxane can be unthreaded by the addition of tetrabutylammonium chloride because of the formation of a strong ion pair of dialkylammonium chloride, whereas the pseudorotaxane structure is regenerated upon addition of tributylammonium hexafluorophosphate.[5] We speculated that by combining these features we might achieve a reversible fabrication of SHPs on the basis of the above acid–base or ion-pairing reactions, which would be accompanied by a controllable fluorescence switch.

To this end, we synthesised a π-conjugated AB_2 monomer **1** with a DB24C8 ring and two secondary amine centres (Figure 1 and Scheme 1). The reasons for selecting **1** were threefold. 1) On treating a solution of **1** in dichloromethane

[a] B. Yu, Dr. B. Wang, S. Guo, Q. Zhang, X. Zheng, H. Lei, Prof. Dr. W. Liu, Prof. Dr. W. Bu
Key Laboratory of Nonferrous Metals Chemistry and Resources Utilization of Gansu Province
State Key Laboratory of Applied Organic Chemistry and College of Chemistry and Chemical Engineering
Lanzhou University, Lanzhou, Gansu, 730000 (P.R. China)
Fax: (+86) 9318912582
E-mail: buwf@lzu.edu.cn

[b] Y. Zhang, Dr. X. Chen
National Laboratory for Infrared Physics
Shanghai Institute of Technical Physics
Chinese Academy of Sciences, Shanghai, 200083 (P.R. China)

Supporting information for this article is available on the WWW under http://dx.doi.org/10.1002/chem.201204315.

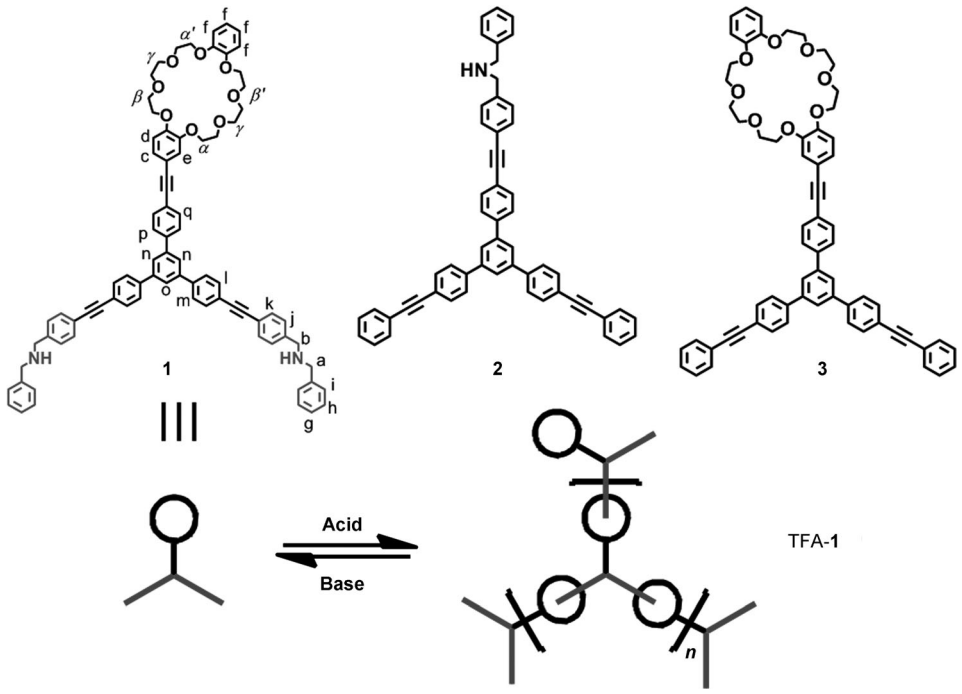

Figure 1. Top: Chemical structures of the AB_2 monomer **1** and model molecules **2** and **3**. Bottom: Schematic representation of the reversible formation of the SHP, TFA-**1**.

with trifluoroacetic acid (TFA), strong host–guest interactions between the dialkylammonium ion centres and DB24C8 groups resulted in formation of the SHP TFA-**1**, which could be subsequently depolymerised by adding excess *N-tert*-butyl-*N*′,*N*′,*N*″,*N*″,*N*‴,*N*‴-hexamethylphosphorimidic triamide (P_1-*t*Bu), tetrabutylammonium fluoride (TBAF), or tetrabutylammonium acetate (TBAOAc). 2) The large distance between the secondary dialkylammonium and DB24C8 groups excludes the possibility of intramolecular recognition in the protonated monomer. 3) The rigid triangular structure of **1** is highly fluorescent[6] and thus the reversible formation of TFA-**1** is accompanied by a reversibility in intensity of both the monomeric and excimeric emissions.

Results and Discussion

The AB_2 monomer **1** and the model compounds **2** and **3** (Figure 1) were synthesised according to the routes depicted in Scheme 1, and Schemes S1 and S2 in the Supporting Information, respectively. The intermediate **8** was synthesised by three Sonogashira cross-coupling reactions starting from 1,3,5-tris(4′-iodophenyl)benzene (**4**);[7] other reactants such as 4-formylphenylacetylene[8] and **7**[9] were synthesised as described previously. The imine **9** was obtained by treating **8** with benzylamine. Reduction of the imine with sodium borohydride generated the final product **1**. The model molecules **2** and **3** were synthesised in a similar manner. They were characterised by their high-resolution electrospray ionisation mass spectra (ESI-MS) and ^{1}H and ^{13}C NMR spectra. The supramolecular polymerisation of AB_2 monomer **1** to the SHP TFA-**1** was monitored by ^{1}H NMR spectroscopy, matrix-assisted laser desorption/ionisation time-of-flight mass spectrometry (MALDI-TOF-MS), solution viscosity, dynamic light scattering (DLS),

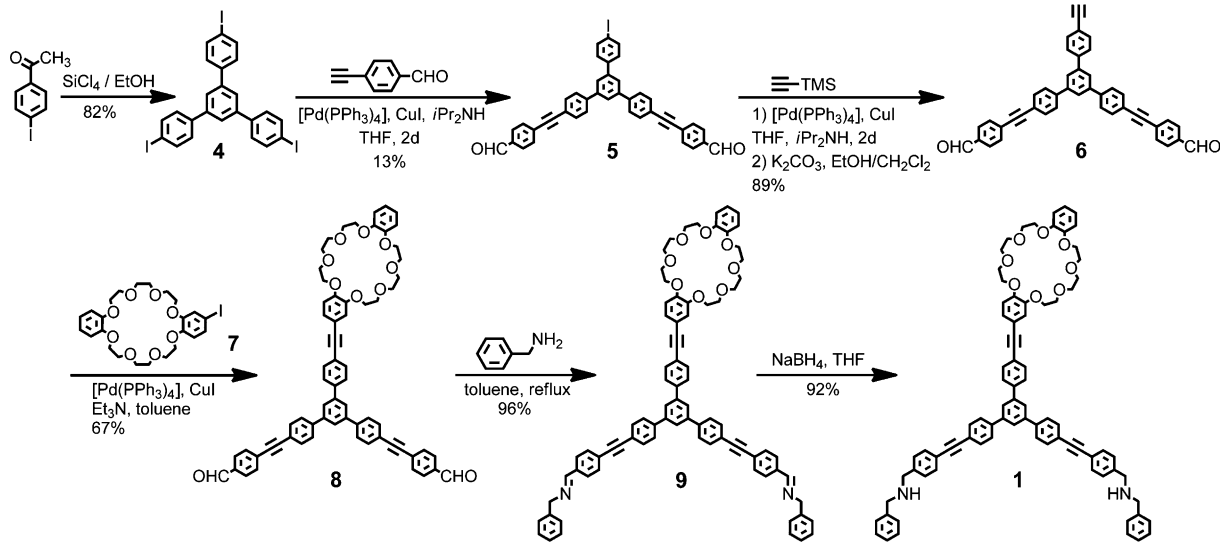

Scheme 1. The synthetic route to AB_2 monomer **1** (TMS = trimethylsilyl).

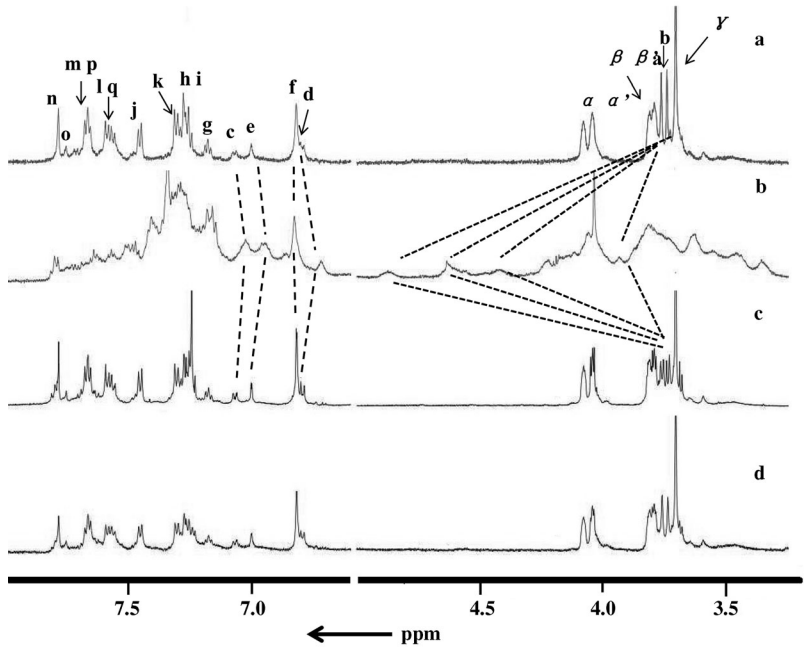

Figure 2. ^{1}H NMR spectra (600 MHz, in CD_2Cl_2, 5.0×10^{-4} mol L^{-1}) of a) **1**, b) TFA-**1** produced by adding 2.2 equivalents of TFA to the solution of **1**, c) **1** obtained by treating TFA-**1** with 2.4 equivalents of P_1-*t*Bu, and d) $\mathbf{1}H_2^{2+}F_2^{2-}$ obtained by treating TFA-**1** with 2.4 equivalents of TBAF.

transmission electron microscopy (TEM), and scanning force microscopy (SFM).

The ^{1}H NMR resonance signals of **1** were fully assigned on the basis of ^{1}H–^{1}H COSY spectra recorded from a solution in CD_2Cl_2. Upon addition of a slight excess of TFA (2.2 equiv), significant changes of the ^{1}H NMR spectrum were observed, as shown in Figure 2a,b. With reference to previous ^{1}H NMR studies on host–guest recognition of DB24C8 derivatives with dialkylammonium groups,[3,4] the three broad peaks at $\delta=4.5$, 4.7, and 4.9 ppm could be unequivocally assigned to the benzylic methylene protons adjacent to the NH_2^+ centres hosted by the DB24C8 moieties (H_{ac}+H_{bc}), whereas the broad signal at $\delta=3.8$–3.9 ppm could be assigned to the methylene protons adjacent to the uncomplexed ammonium groups. The characteristic ^{1}H NMR signals of the crown ether between $\delta=3.2$ and 4.3 ppm were much broader and more complicated than the corresponding peaks before the acid treatment, resembling those observed in supramolecular "daisy chains".[3d] Furthermore, the resonances of the conjugated core were broadened and significantly upfield shifted relative to those of **1**. These shifts and the signal broadening indicated that the the crown ether moieties were threaded by the dialkylammonium ions, confirming the formation of the SHP TFA-**1** upon treatment of **1** with 2.2 equivalents of TFA. It is noteworthy that the resonances of the conjugated core were shifted upfield, which revealed rather strong π–π stacking interactions in TFA-**1**.[3f] Indeed, it was this strong π–π stacking interaction between the conjugated cores that promoted the formation of TFA-**1**, as discussed below. As a result, the resonance signals of the conjugated core were significantly broadened.

The broad resonances of both H_d and H_{ac}+H_{bc} were essentially independent of the others, as shown in Figure 2b. Therefore, the percentage recognition (p) and polymerisation degree (n) could be determined according to Equation (1) in which $A(H_d)$ and $A(H_{ac}+H_{bc})$ are the average integrals of H_d and H_{ac}+H_{bc}, respectively. The values of p and n were estimated to be 98.8± 0.2% and 82±12, respectively, at a concentration of 1.0×10^{-3} mol L^{-1} and 98.5±0.2% and 66±10, respectively, at 5.0×10^{-4} mol L^{-1}. They corresponded to molecular weights of $(1.2\pm0.2)\times10^5$ and $(9.5\pm1.4)\times10^4$ g mol^{-1}, respectively. According to the integrals of the broad peaks at $\delta=4.5$ (linear units), 4.7 (terminal units), and 4.9 ppm (dendritic units), the degrees of branching (DB) were estimated to be 64.0±6.4% at a concentration of 1.0×10^{-3} mol L^{-1} and 66.6±6.6% at 5.0×10^{-4} mol L^{-1}, respectively, on the basis of Equation (2).[1c]

$$p=\frac{n}{(n+1)}=\frac{A(H_{ac}+H_{bc})}{4A(H_d)} \quad (1)$$

$$DB=\frac{[(\text{no. of dendritic units})+(\text{no. of terminal units})]}{(\text{total no. of units})} \quad (2)$$

A further decrease in the concentration would have led to a large error in the calculated values of p and n because of the weaker ^{1}H NMR signals. Upon addition of 2.4 equivalents of P_1-*t*Bu to the same solution, the chemical shifts of the ^{1}H NMR signals in the spectrum obtained (Figure 2c) were essentially consistent with those in the original spectrum, indicating that the formation of TFA-**1** seemed to be nearly reversible. The difference was that the new spectrum displayed sharper and better resolved signals. The resonances of the methylene protons H_a and H_b were changed from singlets at $\delta=3.81$ and 3.83 ppm to doublets at $\delta=3.81$ ($^2J(H,H)=7.2$ Hz) and 3.83 ppm ($^2J(H,H)=7.2$ Hz). The signal of the aromatic proton H_d was clearly observed at $\delta=$ 6.87 ppm with a coupling constant of $J=8.4$ Hz. These clearer resonance signals after an acid–base switching cycle could be attributed to a weakened π–π stacking interaction of **1** in the solution containing the generated TFA·P_1-*t*Bu salt, which was further supported by fluorescence spectroscopic studies (see below).

The MALDI-TOF mass spectrum of TFA-**1**, utilising ditranol as a matrix, further supported the formation of oligomeric species in the gas phase (Figure S1 in the Supporting Information). Peaks attributable to monomeric species appeared at *m*/*z* 1238.1 ($[\mathbf{1}+Na]^+$) and 1329.1 ($[\mathbf{1}+2H+CF_3COO]^+$). Peaks at *m*/*z* 2252.3 and 2342.8 were tentatively attributed to the tetramers $[\mathbf{1}_4+3H+CF_3COO\text{-}4PhCH_2\text{-}2C_6H_5CH_2NH]^{2+}$ and $[\mathbf{1}_4+3H+CF_3COO\text{-}C_6H_5\text{-}2C_6H_5CH_2NH]^{2+}$, respectively, whereas the peak at *m*/*z* 2432.1 was assigned to the dimer $[\mathbf{1}_2+3H+2CF_3COO\text{-}3PhCH_2NH\text{-}C_6H_5CH_2NHCH_2]^+$. Further evidence for the formation of TFA-**1** was provided by viscosity measurements made at 18 °C. The reduced viscosity of solutions of **1** in dichloromethane remained almost constant with increasing concentration (Figure 3a). Upon treating such a solution with 2.2 equivalents of TFA, the reduced viscosity was remarkably enhanced and increased with increasing concentration (Figure 3b). This sharp contrast was consistent with formation of the SHP of TFA-**1** and thus an increase in the size of TFA-**1** with the concentration. A DLS plot of a solution of **1** in dichloromethane (1×10^{-3} mol L^{-1}) showed a peak at a hydrodynamic diameter (D_h) of 1.3 ± 0.2 nm (Figure 3c), which was consistent with its molecular size. After adding 2.2 equivalents of TFA to this solution, two modes were observed at $D_h=324\pm16$ nm and 8885 ± 444 nm (Figure 3d). The former revealed formation of the SHP of TFA-**1**, whereas the latter corresponded to multi-aggregate associates of the SHP. Similar results were obtained for the supramolecular polymer prepared from [60]fullerene with concave aromatic electron donors.[2b] When the same solution was treated with 2.4 equivalents of P_1-*t*Bu, D_h reverted to 1.2 ± 0.2 nm (Figure 3e), demonstrating once again the reversible formation of TFA-**1**. The size and morphology of TFA-**1** were further examined by TEM and SFM. Solutions of TFA-**1** were drop-cast onto carbon-coated copper grids for TEM observation. To obtain clear images, the cast films of TFA-**1** were stained with RuO_4 vapour. Typical images showed that spherical aggregates coexisted with crescent-shaped aggregates (Figure 4a,b). Their respective diameters were estimated to be 115 ± 15 and 800 ± 50 nm at a concentration of 1×10^{-3} mol L^{-1}, smaller than the values obtained from the DLS measurement. This was most probably due to the swelling behaviour of the supramolecular aggregates in solution. On decreasing the concentration to 8×10^{-6} mol L^{-1}, both TEM (Figure 4c) and SFM images (Figure 4d) revealed that TFA-**1** formed spherical aggregates with diameters in the range 18–65 nm. The decreasing degree of polymerisation and size of TFA-**1** with decreasing concentration was consistent with the aforementioned viscosity measurements and previous findings for other SHPs[2] and supramolecular polymers.[10] Even when the concentration was decreased to the order of 10^{-6} mol L^{-1}, TFA-**1** still formed spherical aggregates with a diameter of several tens of nanometers. The MALDI-TOF MS, viscosity, and DLS results, as well as the microscopy images, were consistent with the formation of TFA-**1** as revealed by the ^{1}H NMR spectra.

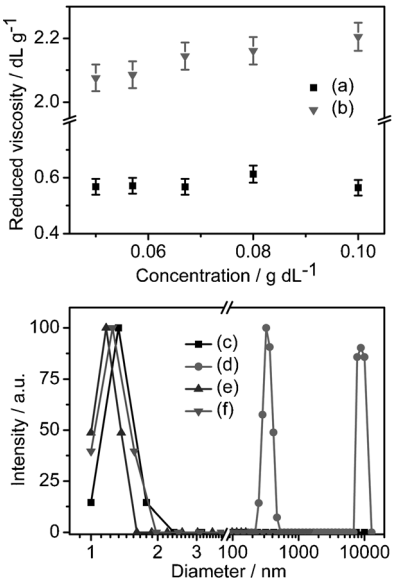

Figure 3. Reduced viscosity as a function of the concentration of a) **1** and b) TFA-**1** in dichloromethane at 18 °C. DLS plots of c) **1** (in CH_2Cl_2, 1.0×10^{-3} mol L^{-1}), d) TFA-**1** produced by adding 2.2 equivalents of TFA into a solution of **1**, e) **1** obtained by treating TFA-**1** with 2.4 equivalents of P_1-*t*Bu, and f) $\mathbf{1}H_2^{2+}F_2^{2-}$ obtained by treating TFA-**1** with 2.4 equivalents of TBAF.

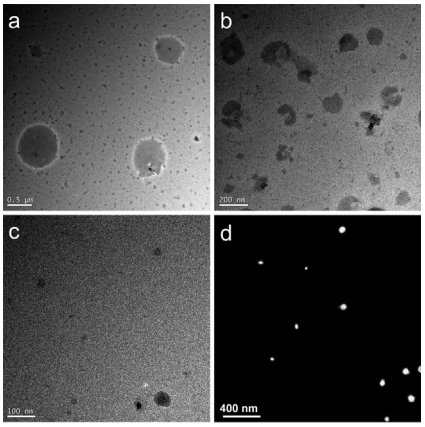

Figure 4. TEM images of TFA-**1** as drop-cast onto carbon-coated copper grids at concentrations of a,b) 1×10^{-3} mol L^{-1} and c) 8×10^{-6} mol L^{-1}. d) SFM image of TFA-**1** as drop-cast onto a silicon substrate at a concentration of 8×10^{-6} mol L^{-1}.

To further support the formation of TFA-**1**, we studied the binding of the model compounds **2** and **3** under acidic conditions. Upon adding a slight excess of TFA (1.1 equiv) to a mixed solution containing **2** and **3** in a molar ratio of 1:1 (total concentration: 1.0×10^{-3} mol L^{-1}), two distinct broad peaks appeared at $\delta=4.6$ and 4.7 ppm in the ^{1}H NMR spectrum, indicative of formation of the host–guest complex $[\mathbf{2}\cdot\mathbf{3}\cdot\mathbf{H}]^+TFA^-$ (Figure S2 in the Supporting Information). The resonances of both the conjugated core and crown ether in $[\mathbf{2}\cdot\mathbf{3}\cdot\mathbf{H}]^+TFA^-$ were similarly broadened and

shifted as those for TFA-**1**, albeit to a much lesser extent (Figure 2b and Figure S2b in the Supporting Information). This difference may be attributed to the formation of TFA-**1** being favoured by much stronger π–π stacking interactions between the conjugated cores. The signal at $\delta = 7.78$ ppm due to the central aromatic protons was not overlapped with others, and could therefore be used as an internal reference to determine the yield of [**2·3·H**]$^+$TFA$^-$. The ratio of the integral of the signal at $\delta = 7.78$ ppm to that of the signals at $\delta = 4.6$ and 4.7 ppm was estimated to be about 1:1, which was consistent with the corresponding value in the original spectrum. This indicated quantitative formation of [**2·3·H**]$^+$ TFA$^-$. After adding 1.2 equivalents of P_1-*t*Bu to the same solution, the ^{1}H NMR spectrum obtained (Figure S2c in the Supporting Information) was essentially consistent with the original one, indicating that the formation of the model complex [**2·3·H**]$^+$TFA$^-$ was pH-controlled and completely and quantitatively reversible. A similar situation was evident at a total concentration of 5.0×10^{-4} mol L^{-1}. The formation of [**2·3·H**]$^+$TFA$^-$ was further confirmed by the ESI mass spectrum, which featured a new peak at *m*/*z* 1073.7187 due to [**2·3·H**]$^+$ (*m*/*z* calculated 1073.7164 (Figure S3 in the Supporting Information)).

With these results in mind, we proceeded to investigate how the fluorescence behaviour of the solutions was influenced by the reversible formation of the SHP and thus the controllable presence of π–π stacking interactions between the conjugated cores. The electronic absorption spectra of both **1** and TFA-**1** showed a π–π* band centred at 315 nm. Upon excitation at this wavelength, a solution of **1** in dichloromethane (8×10^{-6} mol L^{-1}, Figure 5a) exhibited a strong fluorescence band at $\lambda_{max} = 393$ nm together with a shoulder near 480 nm. Upon dropwise addition of TFA, the fluorescence band at 393 nm showed a stepwise decrease in intensity, which was accompanied by a slight increase in intensity of the shoulder band near 480 nm. These changes reached their greatest extents at a TFA/**1** molar ratio of around 2 (Figure 5b). Of note was that the fluorescence band at 393 nm for **1** was shifted toward lower energy, appearing at 400 nm for TFA-**1**, indicative of a slight modification of the electronic conformation by [N$^+$–H···O] and [C–H···O] hydrogen bonds. The resulting solution of TFA-**1** was further titrated with P_1-*t*Bu. The titration data showed that the fluorescence intensities of the bands at both 393 and 480 nm reverted to the original levels for **1** at a P_1-*t*Bu/TFA-**1** molar ratio of 2 (Figure S4 in the Supporting Information and Figure 5c). However, no change was observed in the UV/Vis absorption spectrum. Taking these features together, the bands at 393 and 400 nm were assigned to the monomeric emissions of **1** and TFA-**1**, respectively, whereas the band at 480 nm was assigned to an excimeric emission. The fluorescence enhancement of the excimeric emission at 480 nm could be attributed to the much stronger π–π stacking interaction in TFA-**1** compared to that in **1**, as revealed by their ^{1}H NMR spectra. In sharp contrast, the fluorescence intensity of [**2·3·H**]$^+$TFA$^-$ was largely unaffected by the host–guest recognition (Figure S5 in the Supporting Information), which was consistent with the much narrower ^{1}H NMR signals and thus a much weaker π–π stacking interaction in [**2·3·H**]$^+$TFA$^-$ compared to that in TFA-**1**. Figure 5c illustrates a reversible intensity change of the fluorescence band at 393 nm upon successive additions of TFA and P_1-*t*Bu, albeit with partial loss of the signal in the first cycles. The fluorescence intensities after repeated treatment with P_1-*t*Bu were quite consistent with the original intensity of **1**. TFA-**1** showed a stepwise increase in its fluorescence intensity, which reached a maximum after seven acid/base cycles. Further alternate additions of acid and base to the solution yielded reversible cycles of fluorescence changes with almost no loss of the signal intensity.

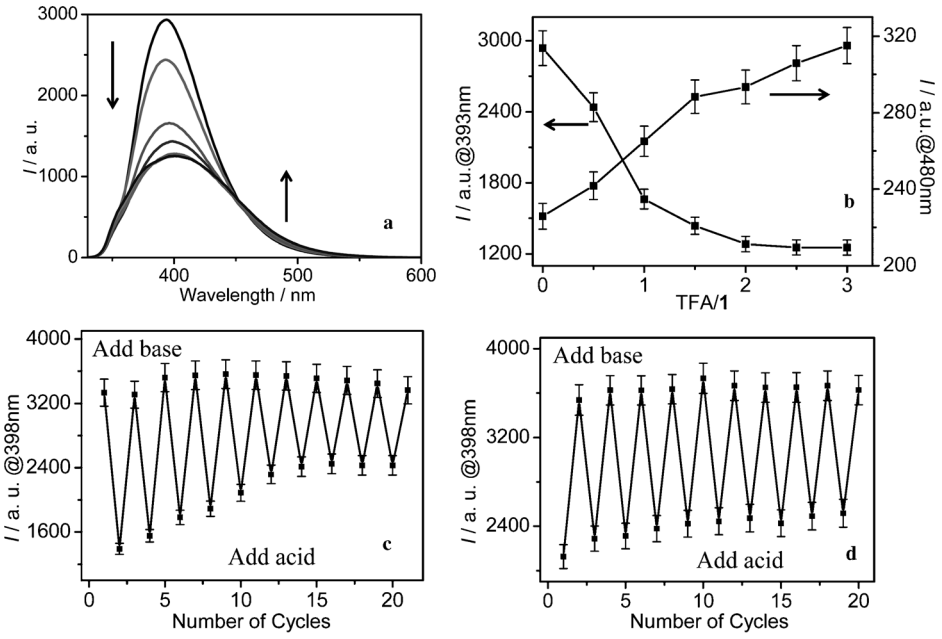

Figure 5. a,b) Fluorescence spectral changes of **1** (8×10^{-6} mol L^{-1}, dichloromethane) upon titration with TFA (TFA/**1** = 0, 0.5, 1, 1.5, 2.0, 2.5, 3.0) at both the monomeric and excimeric emission bands. Fluorescence intensity changes of **1** at 393 nm in c) dichloromethane and d) dichloromethane containing 50 equivalents of TFA·P_1-*t*Bu upon alternate additions of TFA and P_1-*t*Bu for ten repeating cycles.

The TFA$^-$ ion can form a strong ion pair with the dibenzylammonium cation, so much so that even host–guest recognition between DB24C8 and dibenzylammonium is inhibited in solvents of low dielectric constant.[4h,i] However, quantitative recognition was observed in solutions of both TFA-**1** and [**2·3·H**]$^+$TFA$^-$ in

dichloromethane, which may be attributed to a cooperative combination of strong π–π stacking interactions between the π-conjugated molecules, as revealed by their broadened and upfield-shifted ^{1}H NMR signals, together with [N$^+$–H···O] and [C–H···O] hydrogen bonds. A high concentration of TFA$^-$ can completely suppress the host–guest recognition of dibenzylammonium with DB24C8 in media of low polarity.[4i] However, in the present case, such recognition still occurred even after ten acid/base cycles, which may have been due to a rather high binding constant of TFA with P$_1$-*t*Bu (pK_b = 26.5).[3f,11] The partial loss of the fluorescence signals (Figure 5c) may be attributed to the presence of traces of free TFA$^-$ in an ion-paired solution of TFA•P$_1$-*t*Bu produced by the acid–base switching process. To further prove this effect, a solution of **1** in dichloromethane (8×10^{-6} mol L^{-1}) containing 50 equivalents of TFA•P$_1$-*t*Bu was prepared, which showed a fluorescence intensity consistent with that of **1** at the same concentration. After adding 2.2 equivalents of TFA, the fluorescence intensity at 393 nm decreased, becoming similar to that of TFA-**1** after it had been subjected to seven acid/base cycles (Figure 5d). With successive additions of P$_1$-*t*Bu and TFA to this solution, the increases and decreases in the emission at 393 nm were reversible over at least ten cycles with almost no loss of the signal intensity (Figure 5d). This phenomenon might be attributable to the almost constant concentration of TFA$^-$ originating from the ion-pairing effect and activity coefficient in a solution with such a high ionic strength as TFA•P$_1$-*t*Bu.[4i]

Due to the different excitation properties of **1** and TFA-**1**, we measured the lifetimes of both the monomeric and excimeric bands at 393 and 480 nm, respectively, upon excitation at 315 nm. The fluorescence decay profiles were well-fitted by double-exponential curves, with the lifetimes being essentially independent of the emission wavelengths of 393 nm (Table 1 and Figure S6 in the Supporting Information) or 480 nm (Table S1 and Figure S7 in the Supporting Information). When 2.2 equivalents of TFA were added to a solution of **1** to form TFA-**1**, the faster component of $\tau = 1.10\pm0.11$ ns showed a decrease in its relative weighting from 92.25 ± 4.61 % to 53.77 ± 2.67 %, whereas the relative contribution of the longer-lifetime component of 5.23 ± 0.52 ns was found to increase from 7.75 ± 0.39 % to 46.23 ± 2.31 %. Basically, the fluorescence lifetimes reverted to their original values for **1** after treating a solution of TFA-**1** in dichloromethane with 2.4 equivalents of P$_1$-*t*Bu. A solution of **1** in dichloromethane containing 50 equivalents of TFA•P$_1$-*t*Bu showed a fluorescence decay similar to that of **1**. With the formation of TFA-**1** by adding 2.2 equivalents of TFA to this solution, the relative contributions of the shorter- and longer-lifetime components were estimated to be 74.78 ± 3.74 % and 25.22 ± 1.26 %, respectively, and were again restored to their original values for **1** after the addition of a slight excess of P$_1$-*t*Bu. These reversible fluorescence decays were fully consistent with the intensity changes of the emission bands at both 393 and 480 nm. On the basis of these data, the lifetimes of 1.10 ± 0.11 and 5.23 ± 0.52 ns could be unequivocally assigned to the monomeric and excimeric emissions, respectively.

Table 1. Luminescence lifetimes[a] (τ_1 and τ_2) for **1** and TFA-**1**.

Sample	τ_1 [ns]	RW$_1$ [%][b]	τ_2 [ns]	RW$_2$ [%][b]
1	1.10 ± 0.11	92.25 ± 4.61	5.23 ± 0.52	7.75 ± 0.39
TFA-**1**[c]	1.39 ± 0.14	53.77 ± 2.67	5.97 ± 0.60	46.23 ± 2.31
1[d]	1.05 ± 0.10	94.12 ± 4.71	4.92 ± 0.49	5.88 ± 0.29
1[e]	1.06 ± 0.11	91.39 ± 4.57	4.42 ± 0.44	8.61 ± 0.43
TFA-**1**[f]	1.10 ± 0.11	74.78 ± 3.74	4.93 ± 0.49	25.22 ± 1.26
1[g]	0.99 ± 0.10	94.12 ± 4.71	4.83 ± 0.48	5.88 ± 0.29

[a] 8×10^{-6} mol L^{-1} solutions in CH_2Cl_2 monitored at 393 nm upon excitation at 315 nm. [b] Relative weighting (RW) of components in double-exponential fits. [c] Produced by adding 2.2 equivalents of TFA to a solution of **1**. [d] Obtained by treating TFA-**1** with 2.4 equivalents of P$_1$-*t*Bu. [e] 8×10^{-6} mol L^{-1} solution in CH_2Cl_2 together with 50 equivalents of TFA•P$_1$-*t*Bu. [f] Produced by adding 2.2 equivalents of TFA to the solution in e. [g] Obtained by adding 2.4 equivalents of P$_1$-*t*Bu to the solution in f.

Next, we investigated the fluorescence responsiveness of TFA-**1** towards various anions by means of fluorimetric titrations. The fluorescence intensity at 393 nm increased upon dropwise addition of TBAF and reached a maximum value at a TBAF/TFA-**1** molar ratio of 2:1 (Figure 6a), which was fully consistent with that of **1** in dichloromethane (8×10^{-6} mol L^{-1}). The anionic responsiveness was further confirmed by the ^{1}H NMR spectrum (Figure 2d) and DLS measurement (Figure 3f). Upon addition of 2.4 equivalents of TBAF to the solution of TFA-**1**, the resulting ^{1}H NMR spectrum was completely consistent with that of **1** (Figure 2d). A similar result was obtained upon addition of TBAOAc to a solution of TFA-**1** (Figure S8 in the Supporting Information). These results indicated that the additions of TBAF and TBAOAc led to the formation of the strong ion pairs $\mathbf{1}H_2^{2+}F_2^{2-}$ and $\mathbf{1}H_2^{2+}(OAc)_2^{2-}$, respectively, which led to dissociation of the dialkylammonium cations from the DB24C8 groups. When various other anions, namely, Cl$^-$, Br$^-$, I$^-$, BF_4^-, ClO_4^-, $H_2PO_4^-$, HSO_4^-, NO_3^-, and PF_6^-, were added to a solution of TFA-**1**, however, no significant fluorescence enhancement was detected (Figure 6b). The results showed that F$^-$ and OAc$^-$ have much stronger ion-pairing interactions with dialkylammonium cations than the other anions.

Although the additions of 2.4 equivalents of the aforementioned anions to a solution of TFA-**1** did not produce a significant change of the fluorescence intensities, upon subsequent addition of 2.4 equivalents of TBAF to the solution, the fluorescence intensity was essentially consistent with that of **1** (Figure 6c). However, in such a competitive experiment with TBAOAc, the fluorescence intensity was only partially recovered (Figure S9a in the Supporting Information). This contrasting result revealed that the binding of TFA-**1** with fluoride was highly selective. However, upon successive additions of TFA and TBAF or TFA and TBAOAc, the fluorescence signals were completely lost after five TFA/TBAF or three TFA/TBAOAc cycles, which may be attributed to rather strong ion-pairing effects of F$^-$ or OAc$^-$ and TFA$^-$ with the dialkylammonium cations (Figure 6d and Figure S9b in the Supporting Information). This

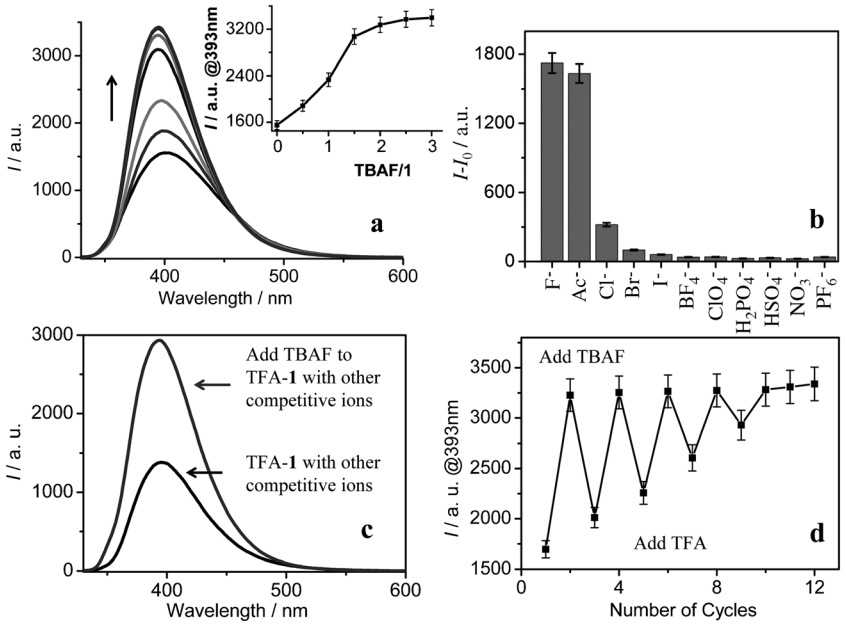

Figure 6. a) Fluorescence spectral changes of TFA-**1** produced by adding 2.2 equivalents of TFA to a solution of **1** (8×10^{-6} mol L^{-1}, dichloromethane) upon titration with TBAF (TBAF/**1** = 0, 0.5, 1, 1.5, 2.0, 2.5, 3.0). b) Fluorescence response ($I-I_o$) of TFA-**1** upon addition of 2.2 equivalents of various anion salts. c) The selectivity of TFA-**1** for F^- in the presence of other anions and d) with alternate additions of TBAF and TFA for five repeating cycles.

situation is markedly different to that controlled by TFA/P_1-*t*Bu cycles (Figure 5c,d), whereby a reversible change in the fluorescence intensity was clearly observed, albeit with some loss of the signal within the first cycles.

Conclusion

We have fabricated a supramolecular hyperbranched polymer (SHP), denoted as TFA-**1**, by adding a slight excess of TFA to a solution of the AB_2 monomer **1** in dichloromethane. The driving force behind its assembly is the host–guest recognition between DB24C8 moieties and dialkylammonium ion centres, together with rather strong π–π stacking interactions between the conjugated cores. The resulting TFA-**1** was depolymerised upon the addition of a slight excess of P_1-*t*Bu or F^-, whereupon the host–guest recognition was lost as a result of deprotonation or a stronger ion-pairing effect involving the ammonium recognition sites. Such acid–base- or ion-pair-controlled fabrication of the SHP induces a reversible change of the fluorescence intensity of the solution due to the controllable presence of π–π stacking interactions between the conjugated cores. Upon successive additions of acid and base to a solution of **1**, reversible changes in the fluorescence intensity were observed over at least ten cycles, after a partial signal loss within the first cycles. The synthesis and characterisation of hyperbranched π-conjugated polymers has attracted much attention recently because of their intriguing physical properties and thus solution-processable applications in a variety of optoelectronic devices.[12] In this context, TFA-**1** can be regarded as a π-conjugated SHP and a dynamic material with controllable π–π stacking interactions between the conjugated cores and thus controllable photophysical properties.

Experimental Section

General considerations: All reaction operations were performed under an anhydrous Ar atmosphere. Anhydrous toluene and tetrahydrofuran (THF) were distilled over Na and benzophenone. Dichloromethane was dried over CaH_2. All chemicals were used as received without any further treatment. ^{1}H and ^{13}C NMR spectra were recorded on Varian 600 MHz or Bruker 400 MHz spectrometers with tetramethylsilane (TMS) as an internal standard. Melting points were determined on a Kofler apparatus. High-resolution ESI mass spectra were obtained on a Bruker APEX II FT-MS mass spectrometer. MALDI-TOF-MS were recorded on an autoflex III smartbeam mass spectrometer (Bruker Daltonics). DLS measurements were performed on a Brookhaven BI-200SM spectrometer. TEM images were acquired with an FEI Tecnai F30 microscope operating at 300 kV. SFM measurements were performed on a commercial Multimode AFM apparatus (Nanoscope IIIa, Veeco Instruments, Santa Barbara) operated in tapping mode. UV/Vis absorption spectra were recorded on a Shimadzu 2550 spectrophotometer. Luminescence measurements were made on a Hitachi F-7000 spectrofluorimeter with a xenon lamp as the excitation source. Fluorescence lifetimes in solution were measured by using a commercially available time-correlated single-photon counting instrument (Edinburgh Instruments, model FL920 CDT) excited with a nanosecond flash lamp. The lifetime data were deconvoluted from the instrumental response and fitted to double-exponential equations.

Synthesis and characterisation

Compound ***5***: 1,3,5-Tris(*para*-iodophenyl)benzene[7] (**4**; 0.68 g, 1.0 mmol), 4-formylphenylacetylene[8] (0.13 g, 1.0 mmol), $[Pd(PPh_3)_4]$ (0.58 g, 0.05 mmol), CuI (19.0 mg, 0.10 mmol), *i*Pr_2NH (0.20 g, 2.0 mmol), and THF (20 mL) were added to a Schlenk tube under an argon atmosphere and the resulting mixture was stirred for 48 h at 50 °C. The crude product was obtained by removing the solvent under reduced pressure, and was then further purified by column chromatography on silica gel (CH_2Cl_2/petroleum ether, 2:1). Compound **5** was isolated as a yellow solid (89 mg, 13% yield). M.p. 119–121 °C; ^{1}H NMR (400 MHz, $CDCl_3$, Me_4Si): δ = 7.45 (d, J(H,H) = 8.4 Hz, 2H), 7.68–7.74 (m, 11H), 7.78 (d, J(H,H) = 1.6 Hz, 2H), 7.84 (d, J(H,H) = 8.0 Hz, 2H), 7.90 (d, J(H,H) = 8.0 Hz, 2H), 10.05 ppm (s, 2H); ^{13}C NMR (100 MHz, $CDCl_3$, Me_4Si): δ = 89.6, 93.2, 93.6, 122.0, 125.2, 127.3, 128.9, 129.1, 129.4, 129.6, 132.1, 132.4, 135.5, 138.0, 140.2, 141.2, 141.6, 141.69, 191.4 ppm; MS (ESI): *m*/*z* calcd for $[C_{42}H_{25}IO_2+H]^+$: 689.0977; found: 689.0989.

Compound ***6***: Compound **5** (0.69 g, 1.0 mmol), trimethylsilylacetylene (0.15 g, 1.5 mmol), $[Pd(PPh_3)_4]$ (0.58 g, 0.05 mmol), CuI (19.0 mg, 0.10 mmol), *i*Pr_2NH (0.20 g, 2.0 mmol), and THF (20 mL) were added to a Schlenk tube under an argon atmosphere and the resulting mixture was stirred for 48 h at 50 °C. The crude product was obtained by removing the solvent under reduced pressure, and was then further purified by column chromatography on silica gel (CH_2Cl_2/petroleum ether, 2:1). A

yellow solid was isolated, which was redissolved in a mixture of EtOH (15 mL) and CH_2Cl_2 (15 mL). K_2CO_3 (1.0 g) was added and the mixture was stirred at room temperature for 3 h. It was then filtered and the solvent was evaporated under reduced pressure. Compound **6** was obtained as a yellow solid (522 mg, 89% yield). M.p. 167–168 °C; ^{1}H NMR (400 MHz, $CDCl_3$, Me_4Si): $\delta = 3.18$ (s, 1H), 7.62–7.74 (m, 16H), 7.80–7.82 (m, 3H), 7.89 (d, J(H,H) = 8.0 Hz, 4H), 10.04 ppm (s, 2H); ^{13}C NMR (100 MHz, $CDCl_3$, Me_4Si): $\delta = 78.2$, 83.4, 89.6, 93.2, 121.6, 121.9, 125.2, 125.3, 127.2, 127.3, 129.5, 129.6, 132.1, 132.4, 132.7, 135.5, 141.0, 141.2, 141.6, 141.7, 191.4 ppm; MS (ESI): m/z calcd for $[C_{44}H_{26}O_2+H]^+$: 587.2011; found: 587.2022.

Compound ***9***: Compounds **6** (0.59 g, 1.0 mmol) and **7**[9] (0.86 g, 1.5 mmol), $[Pd(PPh_3)_4]$ (0.58 g, 0.05 mmol), CuI (19.0 mg, 0.10 mmol), Et_3N (0.20 g, 2.0 mmol), and toluene (20 mL) were added to a Schlenk tube under an argon atmosphere and the resulting mixture was stirred for 72 h at 110 °C. The crude product was obtained by removing the solvent under reduced pressure, and was further purified by column chromatography on silica gel (CH_2Cl_2/MeOH, 20:1). The intermediate **8** was isolated as a brown solid (692 mg, 67%). MS (ESI): m/z calcd for $[C_{68}H_{56}O_{10}+Na]^+$: 1055.3766; found 1055.3813. The intermediate **8** (0.51 g, 0.5 mmol), benzylamine (0.11 g, 1.0 mmol), and toluene (10 mL) were added to a Schlenk tube under an argon atmosphere and the resulting mixture was stirred for 24 h at 110 °C. The solvent was removed under reduced pressure. The crude product was recrystallised from dichloromethane and methanol. Compound **9** was isolated as a yellow solid (581 mg, 96% yield). M.p. 83–87 °C; ^{1}H NMR (400 MHz, $CDCl_3$, Me_4Si): $\delta = 3.83$ (s, 8H), 3.91–3.92 (m, 8H), 4.13–4.15 (m, 8H), 4.83 (s, 4H), 6.81 (d, J(H,H) = 8.4 Hz, 2H), 6.85–6.90 (m, 4H), 7.05 (d, J(H,H) = 1.2 Hz, 1H), 7.12 (d, J(H,H) = 8.4 Hz, 2H), 7.24–7.39 (m, 10H), 7.58–7.69 (m, 16H), 7.76–7.78 (m, 7H), 8.37 ppm (s, 2H); ^{13}C NMR (150 MHz, $CDCl_3$, Me_4Si): $\delta = 65.2$, 69.5, 69.6, 69.9, 70.0, 71.4, 71.5, 88.0, 90.3, 90.6, 91.3, 113.5, 114.2, 185.8, 116.8, 121.5, 122.5, 123.0, 125.1, 125.2, 125.5, 125.6, 127.1, 127.2, 127.3, 127.4, 128.1, 128.1, 128.3, 128.4, 128.5, 128.6, 128.6, 128.7, 131.9, 132.1, 132.3, 135.9, 139.2, 140.3, 140.9, 141.7, 141.9, 161.2 ppm; MS (ESI): m/z calcd for $[C_{82}H_{70}N_2O_8+H]^+$: 1211.5210; found: 1211.5321.

Compound ***1***: Compound **9** (0.12 g, 0.1 mmol), $NaBH_4$ (0.19 g, 0.5 mmol), and THF (10 mL) were added to a Schlenk tube under an argon atmosphere and the resulting mixture was stirred for 24 h at 60 °C. The crude product was obtained by removing the solvent under reduced pressure. Compound **1** was isolated as a yellow solid by recrystallising the crude product from dichloromethane and methanol (112 mg, 92% yield). M.p. 90–93 °C; ^{1}H NMR (400 MHz, $CDCl_3$, Me_4Si): $\delta = 3.81$ (s, 4H), 3.83 (s, 4H), 3.84 (s, 8H), 3.91–3.93 (m, 8H), 4.14–4.17 (m, 8H), 6.82 (d, J(H,H) = 8.4 Hz, 2H), 6.86–6.89 (m, 4H), 7.05 (s, 1H), 7.13 (d, J(H,H) = 8.4 Hz, 2H), 7.24–7.38 (m, 13H), 7.52–7.54 (m, 4H), 7.63–7.70 (m, 12H), 7.77–7.79 ppm (m, 4H); ^{13}C NMR (150 MHz, $CDCl_3$, Me_4Si): $\delta = 53.0$, 53.2, 69.5, 69.6, 69.9, 70.0, 71.4, 71.5, 88.0, 89.2, 90.5, 90.6, 113.5, 114.2, 115.9, 116.8, 121.6, 121.9, 122.9, 123.0, 125.2, 125.5, 126.9, 127.0, 127.1, 127.2, 127.3, 127.4, 128.1, 128.2, 128.3, 128.4, 128.5, 128.6, 128.7, 131.8, 132.1, 132.2, 132.3, 140.2, 140.6, 140.9, 141.8, 141.8, 148.6, 149.0, 149.6 ppm; ^{1}H NMR (600 MHz, CD_2Cl_2): $\delta = 3.74$ (s, 8H), 3.78 (s, 4H), 3.80 (s, 4H), 3.83 (s, 4H), 3.85 (s, 4H), 4.09 (s, 4H), 4.12 (s, 4H), 6.84 (d, J(H,H) = 8.4 Hz, 2H), 6.87 (s, 4H), 7.05 (s, 1H), 7.11 (d, J(H,H) = 8.4 Hz, 2H), 7.22 (dd, J(H,H) = 6.6, 8.4 Hz, 2H), 7.29–7.33 (m, 8H), 7.36 (d, J(H,H) = 7.8 Hz, 4H), 7.50 (d, J(H,H) = 7.8 Hz, 4H), 7.61 (d, J(H,H) = 8.4 Hz, 2H), 7.64 (d, J(H,H) = 7.8 Hz, 4H), 7.71–7.77 (m, 6H), 7.81 (s, 1H), 7.84 ppm (s, 2H); MS (ESI): m/z calcd for $[C_{82}H_{74}N_2O_8+H]^+$: 1215.5518; found: 1215.5530.

Acknowledgements

This work is supported by the National Natural Scientific Foundation of China (20901034, 20931003, and 51173073), the Program for New Century Excellent Talents in University (NCET-10–0462), the Specialized Research Fund for the Doctoral Program of Higher Education (20100211110023), the Fundamental Research Funds for the Central Universities (lzujbky-2012-k14, lzujbky-2011–29, and lzujbky-2010–162), the Gansu Natural Scientific Foundation (1107RJZA214), and the Open Project of State Key Laboratory of Supramolecular Structure and Materials of Jilin University (sklssm201214).

[1] a) C. Gao, D. Yan, *Prog. Polym. Sci.* **2004**, *29*, 183–275; b) B. I. Voit, A. Lederer, *Chem. Rev.* **2009**, *109*, 5924–5973; c) D. Wilms, S. E. Stiriba, H. Frey, *Acc. Chem. Res.* **2010**, *43*, 129–141; d) Y. Zhou, D. Yan, *Chem. Commun.* **2009**, 1172–1188.

[2] a) F. Huang, H. W. Gibson, *J. Am. Chem. Soc.* **2004**, *126*, 14738–14739; b) G. Fernández, E. M. Pérez, L. Sánchez, N. Martín, *J. Am. Chem. Soc.* **2008**, *130*, 2410–2411; c) R. Dong, Y. Liu, Y. Zhou, D. Yan, X. Zhu, *Polym. Chem.* **2011**, *2*, 2771–2774; d) S. Yu, W. Zhang, J. Zhu, Y. Yin, H. Jin, L. Zhou, Q. Luo, J. Xu, J. Liu, *Macromol. Biosci.* **2011**, *11*, 821–827; e) Z. Ge, H. Liu, Y. Zhang, S. Liu, *Macromol. Rapid Commun.* **2011**, *32*, 68–73.

[3] a) P. R. Ashton, P. J. Campbell, E. J. T. Chrystal, P. T. Glink, S. Menzer, D. Philp, N. Spencer, J. F. Stoddart, P. A. Tasker, D. J. Williams, *Angew. Chem.* **1995**, *107*, 1997–2001; *Angew. Chem. Int. Ed. Engl.* **1995**, *34*, 1865–1869; b) A. G. Kolchinski, D. H. Busch, N. W. Alcock, *J. Chem. Soc. Chem. Commun.* **1995**, 1289–1291; c) P. R. Ashton, R. Ballardini, V. Balzani, M. Gómez-López, S. E. Lawrence, M. V. Martínez-Díaz, M. Montalti, A. Piersanti, L. Prodi, J. F. Stoddart, D. J. Williams, *J. Am. Chem. Soc.* **1997**, *119*, 10641–10651; d) S. J. Cantrill, G. J. Youn, J. F. Stoddart, *J. Org. Chem.* **2001**, *66*, 6857–6872; e) K. C.-F. Leung, P. Mendes, M. S. N. Magonov, B. H. Northrop, S. Kim, K. Patel, A. H. Flood, H.-R. Tseng, J. F. Stoddart, *J. Am. Chem. Soc.* **2006**, *128*, 10707–10715; f) J. D. Badjic, C. M. Ronconi, J. F. Stoddart, V. Balzani, S. Silvi, A. Credi, *J. Am. Chem. Soc.* **2006**, *128*, 1489–1499; g) J. Wu, K. C.-F. Leung, D. Beítez, J.-Y. Han, S. J. Cantrill, L. Fang, J. F. Stoddart, *Angew. Chem.* **2008**, *120*, 7580–7584; *Angew. Chem. Int. Ed.* **2008**, *47*, 7470–7474; h) L. Fang, M. Hmadeh, J. Wu, M. A. Olson, J. M. Spruell, A. Trabolsi, Y.-W. Yang, M. Elhabiri, A.-M. Albrecht-Gary, J. F. Stoddart, *J. Am. Chem. Soc.* **2009**, *131*, 7126–7134.

[4] a) H. W. Gibson, N. Yamaguchi, J. W. Jones, *J. Am. Chem. Soc.* **2003**, *125*, 3522–3533; b) T. Oku, Y. Furusho, T. Takata, *Angew. Chem.* **2004**, *116*, 984–987; *Angew. Chem. Int. Ed.* **2004**, *43*, 966–966; c) Z. Ge, J. Hu, F. Huang, S. Liu, *Angew. Chem.* **2009**, *121*, 1830–1834; *Angew. Chem. Int. Ed.* **2009**, *48*, 1798–1802; d) F. Wang, C. Han, C. He, Q. Zhou, J. Zhang, C. Wang, N. Li, F. Huang, *J. Am. Chem. Soc.* **2008**, *130*, 11254–11255; e) Y.-S. Su, J.-W. Liu, Y. Jiang, C.-F. Chen, *Chem. Eur. J.* **2011**, *17*, 2435–2441; f) X.-Z. Zhu, C.-F. Chen, *J. Am. Chem. Soc.* **2005**, *127*, 13158–13159; g) V. Blanco, A. Carlone, K. D. Hänni, D. A. Leigh, B. Lewandowski, *Angew. Chem.* **2012**, *124*, 5256–5259; *Angew. Chem. Int. Ed.* **2012**, *51*, 5166–5169; h) J. W. Jones, H. W. Gibson, *J. Am. Chem. Soc.* **2003**, *125*, 7001–7004; i) H. W. Gibson, J. W. Jones, L. N. Zakharov, A. L. Rheingold, C. Slebodnick, *Chem. Eur. J.* **2011**, *17*, 3192–3206; j) Y. Tachibana, N. Kihara, T. Takata, *J. Am. Chem. Soc.* **2004**, *126*, 3438–3439.

[5] M. Montalti, L. Prodi, *Chem. Commun.* **1998**, 1461–1462.

[6] a) S. Sirilaksanapong, M. Sukwattanasinitt, P. Rashatasakhon, *Chem. Commun.* **2012**, *48*, 293–295; b) J. Pang, E. J.-P. Marcotte, C. Seward, R. S. Brown, S. Wang, *Angew. Chem.* **2001**, *113*, 4166–4169; *Angew. Chem. Int. Ed.* **2001**, *40*, 4042–4045.

[7] S. Kotha, D. Kashinath, K. Lahiri, R. B. Sunoj, *Eur. J. Org. Chem.* **2004**, 4003–4013.

[8] X. Wang, V. Ervithayasuporn, Y. Zhang, Y. Kawakami, *Chem. Commun.* **2011**, *47*, 1282–1284.

[9] S. Dixon, R. C. D. Brown, P. A. Gale, *Chem. Commun.* **2007**, 3565–3567.

[10] a) T. F. A. De Greef, M. M. J. Smulders, M. Wolffs, A. P. H. J. Schenning, R. P. Sijbesma, E. W. Meijer, *Chem. Rev.* **2009**, *109*, 5687–5754; b) B. Zheng, F. Wang, S. Dong, F. Huang, *Chem. Soc. Rev.* **2012**, *41*, 1621–1636; c) Y. Liu, Z. Wang, X. Zhang, *Chem. Soc. Rev.* **2012**, *41*, 5922–5932.

[11] a) I. Kaljurand, A. Kütt, L. Sooväli, T. Rodima, V. Mäemets, I. Leito, I. A. Koppel, *J. Org. Chem.* **2005**, *70*, 1019–1028; b) N. K. Pahadi, H. Ube, M. Terada, *Tetrahedron Lett.* **2007**, *48*, 8700–8703.
[12] a) M. Häußler, B. Z. Tang, *Adv. Polym. Sci.* **2007**, *209*, 1–58; b) J. Wang, J. Mei, E. Zhao, Z. Song, A. Qin, J. Z. Sun, B. Z. Tang, *Macromolecules* **2012**, *45*, 7692–7703; c) P. Taranekar, Q. Qiao, H. Jiang, I. Ghiviriga, K. Schanze, J. R. Reynolds, *J. Am. Chem. Soc.* **2007**, *129*, 8958–8959; d) H. S. Mangold, T. V. Richter, S. Link, U. Würfel, S. Ludwigs, *J. Phys. Chem. B* **2012**, *116*, 154–159; e) Z. Xue, A. D. Finke, J. S. Moore, *Macromolecules* **2010**, *43*, 9277–9282.

Received: December 4, 2012
Published online: February 18, 2013

